Polymer 107 (2016) 122–129

Contents lists available at ScienceDirect

Polymer

journal homepage: www.elsevier.com/locate/polymer

An alternative method for long chain branching determination by triple-detector gel permeation chromatography

Thipphaya Pathaweeisariyakul [a, *], Kanyanut Narkchamnan [a], Boonyakeat Thitisak [a], Wonchalerm Rungswang [a], Wallace W. Yau [b]

[a] SCG Chemicals Co., Ltd., 1 Siam Cement Rd., Bangsue, Bangkok 10800, Thailand
[b] Polymer Characterization Consultant, 7755 Tim Tam Ave., Las Vegas, NV 89178, USA

ARTICLE INFO

Article history:
Received 8 August 2016
Received in revised form
14 October 2016
Accepted 5 November 2016
Available online 8 November 2016

Keywords:
Long chain branch
GPC
Light Scattering

ABSTRACT

Gel permeation chromatography with refractive index (RI) or infrared detector (IR), viscometer for intrinsic viscosity (IV) and/or light scattering (LS) has become a prominent technique for quantitative study of polymer long chain branching (LCB). A quantity known as LCB frequency (LCB*f*) derived from *g*-factor of Zimm-Stockmayer (ZS) model was here studied and found its problems in reproducibility and accuracy. In this work, an alternative high precision method of the gpcBR approach was used to estimate a more reliable *g*-factor, called g_{est}. The branching index, *B*-factor for number of LCB per molecule was found to be more relevant than LCB*f* in relating to polymer properties. A proposal is made that enables the distinction between two LCB categories, i.e. branch on main chain and branch on branch. This allows the analysis of these two LCB types on their relative importance to polymer processing and end-use properties. NMR results were obtained in support of the LCB data.

1. Introduction

In polyethylene technology, long chain branching (LCB) is an important microstructure that affects many processing properties, such as melt viscosity, melt strength, die swell ratio, etc. [1,2] For example, in LDPE extrusion coating process, long chain branching structure can improve neck-in properties [3,4]. To support the polymer design development, a well-defined characterization technique for LCB is required.

Gel permeation chromatography (GPC) or size exclusion chromatography (SEC) has become a prominent technique to determine long chain branching of polymer, in addition to its traditional use for the determination of molecular weight (MW) and molecular weight distribution. The well-known MW-sensitive online detectors coupling with GPC to analyze LCB are multi-angle light scattering (MALS) and intrinsic viscometer (IV), in cooperation with a conventional concentration detector, like refractive index detector (RI) or infrared detector (IR) [2,5–15]. GPC with RI or IR, MALS, and IV, often called 3D-GPC or GPC-3D (GPC with triple detectors), can be used to study polymer LCB. Based on slice by slice calculation, it is possible also to obtain LCB distribution along the polymer molecular weight by using the Zimm-Stockmayer random branching model [7,9,11,16,17]. With the same molecular weight, the root-mean-square radius (R_g) of a branched polymer is smaller than that of a linear polymer. The branching index *g*-factor is defined as the ratio of the R_g square of the branched polymer over that of a linear polymer of same molecular weight, as shown in Equation (1). Similarly, the branching index from intrinsic viscosity, *g*'-factor, is defined as the ratio of intrinsic viscosity ($[\eta]$) of a branched polymer over the $[\eta]$ of linear polymer of same molecular weight, as shown in Equation (2). These two indices are related with an exponent power ε, so called structure factor, as shown in Equation (3).

$$g = \left\langle R^2_{g\ \mathrm{branch}} \right\rangle \Big/ \left\langle R^2_{g\ \mathrm{linear}} \right\rangle \tag{1}$$

$$g' = [\eta]_{\mathrm{branch}} / [\eta]_{\mathrm{linear}} \tag{2}$$

$$g' = g^{\varepsilon} \tag{3}$$

To estimate *g* from *g*', a value of this epsilon (ε) parameter must be assumed. The problem is that, this structure factor can vary from 0.5 to 1.5, depending on molecular architecture [5] and recently it

* Corresponding author.
E-mail address: thipphap@scg.co.th (T. Pathaweeisariyakul).

http://dx.doi.org/10.1016/j.polymer.2016.11.007
0032-3861/

was found to be also depending on degree of polymerization [18,19]. It is even more challenging for LDPE which has very complex branching architectures.

From g value, the number average LCB per molecule (B_n) can be estimated from the Zimm-Stockmayer equation for a monodisperse, tri-functionally branched polymer, Equation (4) [16].

$$g = \left[\left(1+\frac{B_n}{7}\right)^{1/2} + \frac{4B_n}{9\pi}\right]^{-1/2} \quad (4)$$

From the B_n value obtained from Equation (4), the LCBf value for the number of LCB per 1000 carbon can be calculated by using Equation (5).

$$LCBf = \lambda = R \cdot B_n \cdot \frac{1000}{M} = number\ \ of\ \ LCB\ \ per\ \ 1000\ carbon \quad (5)$$

where, M is molecular weight, and R is a factor of the repeating molecular weight unit. For example, polyethylene, $R = (14 + 14)/2 = 14$, or for PVC, $R = (14 + 13{+}35)/2 = 31$.

A new branching approach, gpcBR, has been recently introduced to analyze LCB by 3D-GPC by Yau and co-workers [15,20]. Comparing to the traditional g or g' and LCBf parameter, this new gpcBR index provides a measurement of polymer branching level with a much improved precision. It is the combination of intrinsic viscosity [η] and absolute weight average molecular weight ($M_{W,ABS}$) measured from MALS. The expression of gpcBR is the following:

$$gpcBR = \left[\left(\frac{[\eta]_{CC}}{[\eta]}\right)\cdot\left(\frac{M_{W,ABS}}{M_{W,CC}}\right)^{\alpha} - 1\right] = \left[\left(\frac{kM_{W,ABS}^{\alpha}}{[\eta]}\right)\cdot\left(\frac{M_{V,CC}}{M_{W,CC}}\right)^{\alpha} - 1\right] \quad (6)$$

where $M_{W,CC}$ and $[\eta]_{CC}$ are the weight average molecular weight and intrinsic viscosity from conventional GPC calculation assuming polymer is linear with no LCB. The [η] term is the actual intrinsic viscosity, which is the measured value from the online viscometer, calculated by the viscometer peak area method. $M_{W,ABS}$ is the weight average of absolute molecular weight from LS detector, also calculated by the LS peak area method for high precision. The high precision quality of gpcBR can be credited to the three key attributes in the gpcBR formulation, as can be explained by the two terms in the gpcBR expression in Equation (6). First, all four parameters, [η], $M_{W,ABS}$, $M_{V,\ CC}$, $M_{W,CC}$ are the most reliable measurements from the 3D-GPC technique, [η] and $M_{W,ABS}$ is not the function of the conventional GPC MW or IV calibration or the GPC instrumental brand broadening. Second, the ratio of $M_{V,CC}$ and $M_{W,CC}$ serves as a correction factor for sample polydispersity. Lastly, any ill-effects of conventional calibration and brand broadening can be cancelled out by the ratio of $M_{V,CC}$ over $M_{W,CC}$. The recent work [15] demonstrated that gpcBR provided more reliable LCB results, and can access lower level of LCB than the traditional indices of the g or g' factors. Data in this study will show the large variation of R_g calculation from MALS by using different LS fitting methods on the same raw data. An expression to correlate gpcBR to ZS model will be established. Moreover the LCB topology in term of types and number of branches will be discussed using the new approach. Finally, these LCB results are discussed in connection to the results of NMR [21], and polymer processing properties.

2. Experiment

A commercial low density polyethylene (LDPE), SCG Chemicals, Thailand, was selected to study the precision of $M_{W,ABS}$ and R_g calculation from GPC with online multi-angle light scattering (GPC-MALS) measurement. Around 24 mg of sample was dissolved in 8 ml of 1,2,4-trichlorobenzene at 160 °C for 60 min. Then the sample solution, 200 μl, was injected into the high temperature GPC with triple detectors (Polymer Char, Spain) with flow rate of 0.5 ml/min at 145 °C in column zone and 160 °C in all 3 detectors. The online detectors consist of IR5 MCT detector, viscometer, and an 8-angle light scattering (Wyatt Technology, USA, assembled by Polymer Char) or MALS. IR5 MCT is a filter-based infrared detector, designed for GPC to determine online concentration and chemical composition in polyolefins. Infrared detector is useful as a concentration detector only when applied to polyolefins with aliphatic CH band. The mobile phase must be selected carefully, in order to minimize background signal. The light scattering model is DAWN HELEOS II, the static light scattering with 8 angles, and the 8 photodetector positions are at 32, 44, 57, 72, 90, 108, 126, and 141°, respectively. However, because of detector noise, the smallest angle was generally neglected in all calculations in this report. Laser wavelength (λ_0) is 662 nm, and the value of 0.104 ml/mg for refractive index difference (dn/dc) of the PE in TCB solution was used. The second virial coefficient was negligible ($A_2 = 0$) due to very dilute solution condition of GPC. The absolute molecular weight ($M_{W,ABS}$) and radius of gyration (R_g) were determined from the intercept and slope at low angle of the Debye plot [22]. The data was processed by GPC One® software, Polymer Char, Spain. To evaluate the LCB quantification method in section 3.3, various grades of in-house commercial LDPE were selected to obtain the branching parameters and relate them to the processing property. Another model sample used in this work is a linear HDPE, which is passed several times through the twin screw extruder at 200 °C, Hake, Germany, to generate long chain branching from a combination of thermal degradation and chain extension LCB processes. The samples at even extrusion rounds (2, 4, 6, and 8) were collected for further measured by 3D-GPC.

Die swell ratio was measured by passing the material through a single screw extruder (Thermo Scientific, HAAKE Rheomex OS, Germany) at 190 °C, connected with Capillary Circular Die 2 × 30 Taper and Laser measurement unit. The measurement was performed at the distance of 10 mm from die exit with 5 repetitions.

^{13}C-NMR spectra were recorded by 500 MHz ASCEND™, Bruker, with cryogenic 10 mm probe. TCB was used as a major solvent with TCE-d2 as a locking agent with the ratio of 4:1 by volume. The experiments were done at 120 °C, and the inverse gate ^{13}C (zgig) of pulse program with 90° for pulse angle were used. The delay time ($D1$) was set to 40 s for full-spin recovery. The LCB number for LDPE was done by the concept of primitive core [21].

3. Results and discussion

3.1. Precision of $M_{W,ABS}$ and R_g calculated from GPC-MALS

First, one LDPE sample was selected and measured by GPC-3D. The data from this measurement was then processed on GPC One® platform, Polymer Char. In an online light scattering technique, Debye plot is used to determine $M_{W,ABS}$ and R_g by plotting light scattering intensity versus observation angle at a given concentration, which is normally very dilute for chromatography technique like GPC. To determine $M_{W,ABS}$ and R_g, a Debye plot constructed from LS signal at each retention volume slice can be processed with three different formulas, commonly known as the Zimm, Debye, or Berry method [22]. To observe the effect of the

fitting methods in this report, these 3 methods were used on the same data set collected at 5 selected GPC slices (with 5 different polymer molecular sizes) at retention volume locations of 16.0, 17.0, 18.0, 19.4, and 20.0 ml, corresponding to molecular weight (MW) of approximately 3700, 900, 300, 75 and 50 kg/mol, respectively. Moreover, Debye plot from each individual method involves more variation from different fitting orders, which can be linear (1st order), and polynomial 2nd − 4th orders. The $M_{W,ABS}$ and R_g results from these fitting methods at 6 different retention volumes of GPC-3D are shown in Fig. 1 (a) and 1 (b), respectively.

This graph illustrates that calculation of $M_{W,ABS}$ from MALS provides much better precision than that of R_g. The uncertainty of R_g determination came mainly from noise contained in the LS signal. For highly noise system, the precision will be poorer. Using R_g value might mislead the calculation of other properties or microstructure such as LCB. Since molar mass values were relatively more reliable even at small polymer size, to calculate LCB from Molar mass would provide more robust results (see discussion below in Section 3.2). As demonstrated in Pathaweeisariyakul et al.' work in 2015 [15], long chain branching calculated from gpcBR approach, where Molar mass absolute was used, was more accurate than that from the conventional Zimm-Stockmayer approach, where g was calculated from R_g by MALS in GPC-3D. Nevertheless, ZS model is still applicable with the gpcBR approach to translate g_{est} to branching number (B) and long chain branch frequency (LCBf) as mentioned in Equations (4) and (5).

3.2. Estimation of LCB g-factor (g_{est}) by Flory-Fox theory

In this part, the g-factor estimated from Flory-Fox theory is demonstrated. R_g can be estimated by follow equation (Equation (7)).

Flory-Fox Theory [23].

$$R_{g,est} = \frac{1}{\sqrt{6}} \cdot \left(\frac{[\eta] \cdot M_{W,ABS}}{\phi} \right)^{1/3} \tag{7}$$

where $M_{W,ABS}$ is absolute molecular weight from MALS, $[\eta]$ is intrinsic viscosity and ϕ is Flory's universal constant. The ϕ parameter is the value of Flory's universal constant, ϕ_0, after undergoing a correction for non-theta solvent/temperature conditions according to the theory of Ptitsyn and Éizner: [24].

$$\varphi = \varphi_0 \left(1 - 2.63\zeta + 2.86\zeta^2\right) \tag{8}$$

At theta conditions $\zeta = 0$, while at non-theta conditions it is related to the Mark-Houwink exponent α via

$$\zeta = \frac{2\alpha - 1}{3} \tag{9}$$

where, ϕ_0 is the Flory universal constant. There are many different reported values for this "constant" appeared in the literature. A commonly used value for it is 2.86×10^{23} in the unit of mol^{-1}. The R_g of sample at each retention volume in Fig. 1 were estimated according to Equation (7)–(9), where the Mark-Houwink's exponent α-value equals to 0.725 for linear PE [25]. For the first approximation in this study, the α-value was assumed to be constant at 0.725 for all polymers. The actual intrinsic viscosity at each particular MW was used for calculation. At high molecular weight, the $R_{g,est}$ value, was found to be very close to R_g determined from LS because of the better MALS signal to noise ratio at high MW. The discrepancy between R_g from LS and $R_{g,est}$ was higher at lower MW. One of the reasons is the "late-elution effect" in GPC column that caused an over-estimate of measured R_g by MALS at low MW region [26]. Fig. 2 shows clearly that R_g from MALS at low MW is up-curling. A late elution of even only a very small amount of high MW molecules with very large size can cause this up-curling. This is partly because R_g from MALS is a z-averaged property [27]. Therefore, it is highly biased by the late-eluting large molecules in the midst of low R_g species eluted normally at the high GPC retention volume. While the $R_{g,est}$ value is calculated by using the weight average quantity of $M_{W,ABS}$, therefore it is much less affected by the "late elution effect".

Moreover the exponent value or the slope of the conformation plot of the $R_{g,est}$ is equal to 0.44, which is quite reasonable for a highly branched polymer. On the other hand, the slopes from the different MALS R_g methods are ranging from 0.19 to 0.28, which was even lower than what's expected of a solid sphere structure (slope = 0.33). Such low slope values are highly unlikely to be true for LD samples. They are indicative of the problems of these MALS R_g results. The LDPE topology should not be as densely packed as a solid sphere. The slope of the LDPE conformation plot should not be less than 0.33.

From the definition of g-factor, ratio of R_g at the same M_W expressed in Eq. (12), g-factor can be calculated by replacing Eqs. (10) and (11) into Eq. (12), yielding g_{est} as shown in Eq. (13).

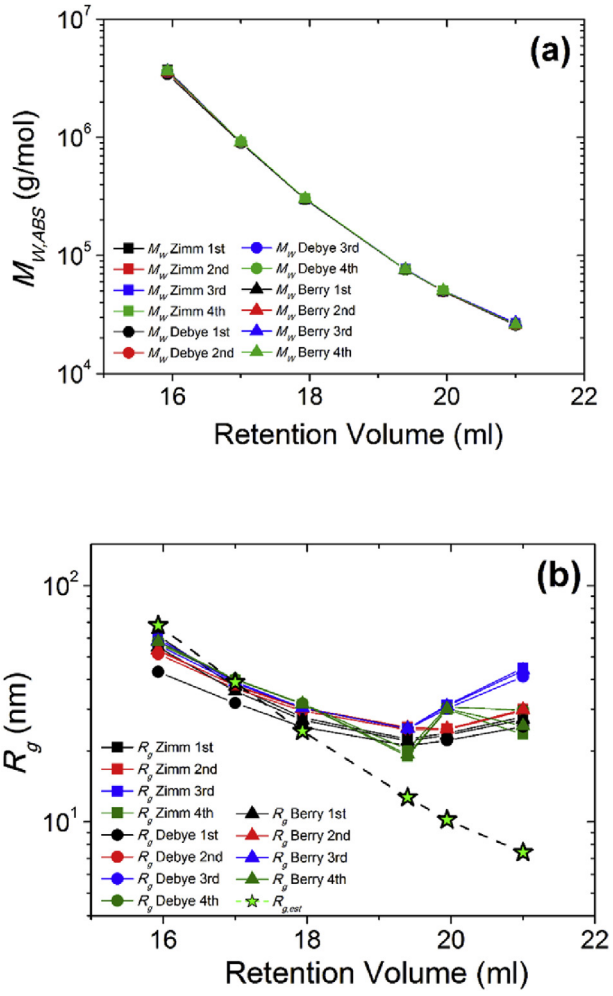

Fig. 1. (a) $M_{W,ABS}$ and (b) R_g calculated from different LS formalisms and various fitting orders from 1st to 4th, Green star represents estimated R_g, $R_{g,est}$. (For interpretation of the references to colour in this figure legend, the reader is referred to the web version of this article.)

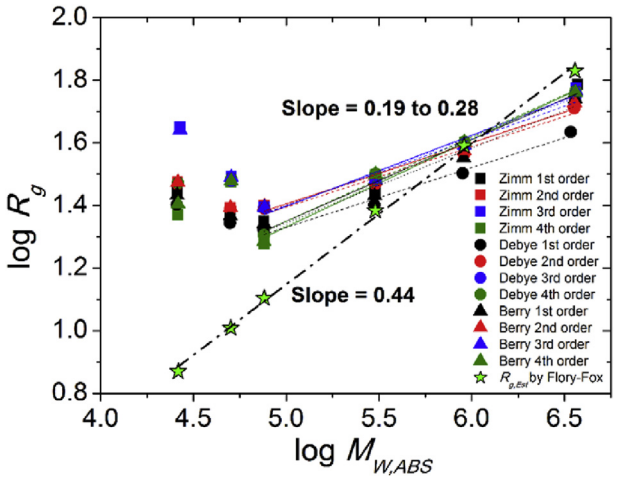

Fig. 2. Conformation plot (log R_g Versus log $M_{W,ABS}$) from different R_g determined by MALS and $R_{g,est}$ by Flory-Fox theory (Green Star). (For interpretation of the references to colour in this figure legend, the reader is referred to the web version of this article.)

$$R_{g,sample,\ est} = \frac{1}{\sqrt{6}} \cdot \left(\frac{[\eta]_{sample} \cdot M_{W,ABS,sample}}{\phi} \right)^{1/3} \tag{10}$$

$$R_{g,linear,\ est} = \frac{1}{\sqrt{6}} \cdot \left(\frac{[\eta]_{linear} \cdot M_{W,ABS,linear}}{\phi} \right)^{1/3} \tag{11}$$

$$g = \frac{R^2_{g,sample}}{R^2_{g,linear}};\ \text{at same } M,\ M_{W,ABS,sample} = M_{W,ABS,linear} = M_{W,ABS} \tag{12}$$

$$g_{est} = \left(\frac{[\eta]_{sample} \cdot M_{W,\ ABS}}{kM^{\alpha}_{W,\ ABS} \cdot M_{W,ABS}} \right)^{2/3} = \left(\frac{[\eta]_{sample}}{kM^{\alpha}_{W,\ ABS}} \right)^{2/3} \tag{13}$$

The gpcBR expression can be derived in term of g_{est} as following,

$$gpcBR = \left[\frac{kM^{\alpha}_{V,CC}}{[\eta]_{sample}} \right] \left[\frac{M_{W,\ ABS}}{M_{W,CC}} \right]^{\alpha} - 1 \tag{14}$$

$$gpcBR + 1 = \left[\frac{kM^{\alpha}_{W,\ ABS}}{[\eta]_{sample}} \right] \left[\frac{M_{V,CC}}{M_{W,CC}} \right]^{\alpha} \tag{15}$$

$$g_{est,gpcBR} = \left(\frac{1}{gpcBR + 1} \right)^{\frac{1}{1.5}} \tag{16}$$

$$PDI\ correction = \left[\frac{M_{V,CC}}{M_{W,CC}} \right]^{2\alpha/3} \tag{17}$$

Note: the presence of the $M_{V,CC}/M_{W,CC}$ factor in Equation (15), and thus in Equation (16)–(17), provides the useful compensation for the sample MW polydispersity to the g_{est} calculation; while the expression of g_{est} in Equation (13) is true in theory only for a monodispersed sample. From Equation (16), $g_{est,gpcBR}$ will be applicable to a polydisperse sample, because gpcBR value already contains the polydispersity correction.

Besides LCB, a commercial LDPE contains also short chain branches (SCB), which can increase local segment density, therefore reduces the intrinsic viscosity. The MH plot will be shifted downward to reduce k value, without substantially changing α-value. In this study, like most others in the literature, no SCB correction was made in calculating the LCB indices, according to several reasons. There is lack of rigorous and generally accepted method that one can use for SCB correction. Any such correction requires several assumptions on the type of SCB and its distribution. Additionally, separated SCB results from NMR or GPC-IR are required. Besides, in many cases, the SCB effects on the LCB calculation were not very significant to begin with. Under these circumstances, making SCB correction is not always recommended in routine GPC LCB calculations. Additional variability can be added to the LCB results at times. Another reason that SCB correction was not included here is because of the purpose of this study. One of the purpose of this study is to show the improved precision of the new proposed LCB method over the traditional MALS R_g method. Since no SCB correction is not made in the traditional MALS R_g method, to obtain a more valid comparison, no SCB correction should be made in our new methods either.

In addition, one should note that there can exist local polydispersity ($M_W/M_N > 1$) in each single GPC slice. That can be the result from instrumental band broadening, which exists at a relatively insignificant level. A larger local polydispersity can happen in analyzing samples containing high level of LCB. A highly branched molecule of higher MW can co-elute with a linear molecule of lower MW, as long as the two molecules have the same hydrodynamic volume, i.e. IV times MW [28–30]. In our LCB calculation, consideration of this topic of great complexity is not accounted for. It is outside the scope and intent of this report.

Fig. 3 shows that the g-factors from various methods are compared. They all show a decrease with increasing molar mass. The blue triangle (▲) is g_{est} from Eq. (13), and the red circle (●) is g_{est} from gpcBR in Eq. (16). Lastly the black upside down triangle (▼) is determined from actual R_g from MALS, which can be calculated only for the last 3 data points due to the problem of up-curling curve of R_g at the two lower MW data points. This problem can even cause R_g of branching polymer to become higher than the R_g of linear polymer. This physically impossible scenario leads to this grossly erroneous situation of the g-factor values being greater than 1, as shown in the inset of Fig. 3.

3.3. Quantification of LCB on the main chain and branch-on-branch

Here, the $g_{est,gpcBR}$, g-factor estimated from gpcBR is used in this

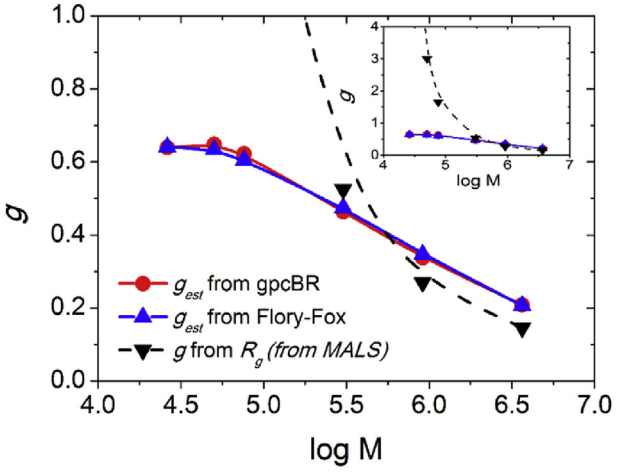

Fig. 3. g -factors calculated by various methods, Inset: g -factor from $R_{g,LS}$ increasing over 1 at low MW due to late-elution effect.

part of study because of its high precision quality. From $g_{est,gpcBR}$, the ZS model is applied to determine branching number, B_n, and long chain branching frequency, LCB*f*. In this part, various grade of LDPE with different gpcBR were selected to study. The overall number of branching, B_{Total}, can be calculated from $g_{est,gpcBR}$ via the ZS model in Eq. (4). The calculation table from gpcBR to $g_{est,gpcBR}$ and B_{Total} is shown in Table 1.

From Table 1, LCB*f* can be calculated from B_{Total} and $M_{W,ABS}$ as shown in Eq. (18). This LCB*f* refers to LCB frequency for the whole molecules, from which we can use Equation (19) to estimate the number of branches on the main chain of the molecule, B_{Main}. In another words, for the complicated LCB structures as in LDPE, the amount of branches on the main chain can be estimated from Eqs. (18) and (19). After the B_{Main} value is determined, the number of branches on branches (B_{BOB}) can be calculated as shown in Eq. (20).

$$LCBf = \frac{14000 \times B_{Total}}{M_{W,\ ABS}} \tag{18}$$

$$LCBf = \frac{14000 \times B_{Main}}{M_{W,CC}} \quad or,\ B_{Main} = LCBf \times M_{W,CC}/14000 \tag{19}$$

$$B_{BOB} = B_{Total} - B_{Main} \tag{20}$$

From the data in Table 1, B_{Total}, B_{Main} and B_{BOB} can be calculated and plotted with gpcBR as shown in Fig. 4. It is clearly seen in this graph that for LDPE sample B_{Main} changes only slightly with gpcBR, while B_{BOB} *increases* considerably with increasing gpcBR.

LCB*f*-R_g and LCB*f*-IV were calculated according to Zimm-Stockmayer model from Eqs. (1)–(5) by using the actual data from GPC-3D. For LCB*f* from IV, to simplify the calculation and avoid adding more errors [15], the short chain branching correction method was not applied here. The ε or structure factor was assumed to be 1.1.

Fig. 5 shows that LCB*f* values of these LDPE sample are nearly constant, independent of gpcBR. That means, LCB*f* parameter in this case failed to be an effective indicator to reflect the difference of low and high LCB levels in the sample. On the other hand, here we show in Fig. 4, the number of branching expressed by the *B* branching factors are much more informative to show the trend of the LCB differences.

To explain the statement above regarding the branching index of the *B*-factor versus LCB*f*, let's consider sample A and sample B illustrated in Fig. 6, for example. Sample A has molecules with one

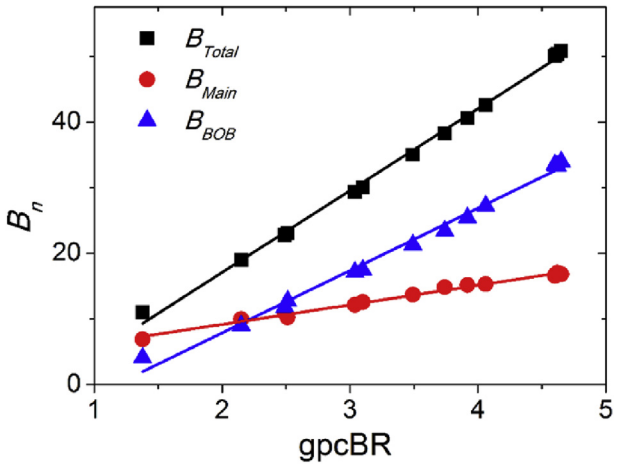

Fig. 4. Branching number (B_n) and gpcBR relationship of LDPE samples.

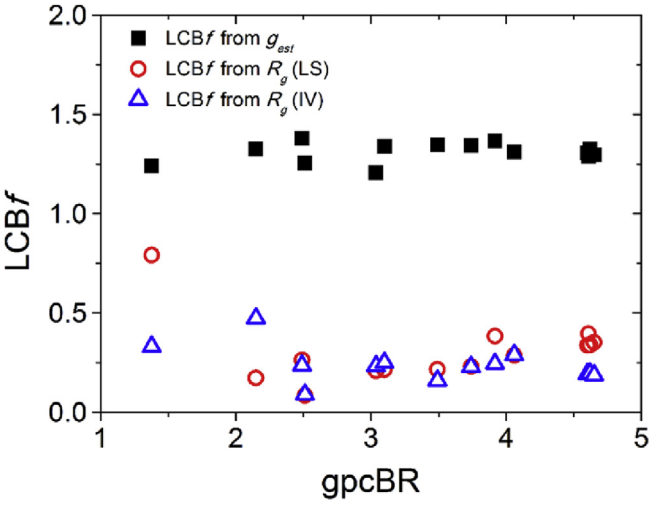

Fig. 5. LCB*f* from g_{est} and LCB*f* from GPC-MALS dependence on gpcBR.

LCB on each molecule, while sample B has two branches on each molecule. But the molecules in sample B is two times bigger than sample A. In this case, the LCB*f* values of sample A and B are equal,

Table 1
GPC-3D data[a] and calculated parameters from various LDPE samples.

Sample	gpcBR Eq. [6]	CH_3/1000C[b] IR5	$M_{W,CC}$ Kg/mol	$M_{W,ABS}$ Kg/mol	$g_{est,gpcBR}$ Eq. [16]	B_{Total} Eq. [4]	LCB*f* $g_{est,gpcBR}$ Eq. [18]	LCB*f*-R_g Eqs. [1], [4] and [5]	LCB*f*- IV Eqs. [2]–[5]	PDI Correction Eq. [17]
A	1.38	17.4	79	125	0.56	11.1	1.24	0.79	0.33	1.09
B	2.15	22.6	106	201	0.47	19.0	1.33	0.17	0.47	1.12
C	2.49	20.8	112	232	0.43	22.8	1.38	0.26	0.24	1.16
D	2.51	24.2	115	257	0.43	23.1	1.26	0.09	0.09	1.13
E	3.04	16.7	142	341	0.39	29.3	1.21	0.21	0.23	1.16
F	3.10	22.6	132	315	0.39	30.1	1.34	0.22	0.25	1.16
G	3.49	21.7	143	364	0.37	35.1	1.35	0.22	0.16	1.16
H	3.74	22.2	155	399	0.35	38.3	1.34	0.23	0.23	1.17
I	3.92	21.8	156	417	0.35	40.7	1.37	0.38	0.25	1.15
J	4.06	20.9	164	455	0.34	42.6	1.31	0.29	0.29	1.17
K	4.60	22.7	178	537	0.32	50.1	1.31	0.34	0.19	1.16
L	4.61	23.7	183	545	0.32	50.2	1.29	0.40	0.19	1.16
M	4.62	22.6	181	533	0.32	50.4	1.32	0.34	0.20	1.17
N	4.65	23.2	182	549	0.32	50.8	1.30	0.35	0.19	1.16

[a] Data error was less than 2% for gpcBR and M_W information, but up to 10% for LCB*f* –R_g and LCB*f*-IV from the previous study [15].
[b] CH_3/1000C from GPR-IR5 represents all methyl groups, including chain ends, and all branches. *From ^{13}C-NMR, total SCB was around 3–4%mol, including methyl, butyl, and hexyl branches for these samples.*

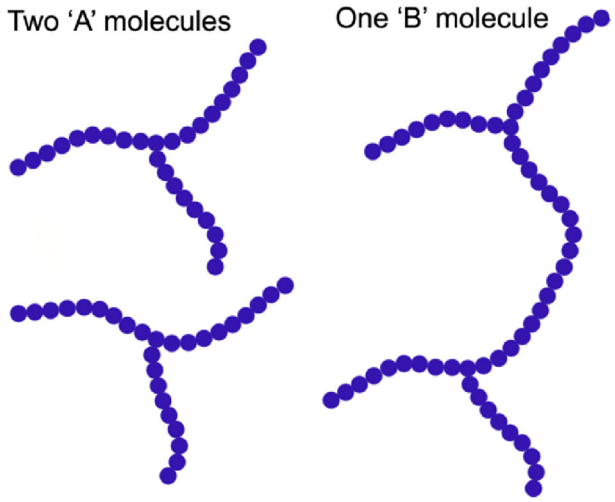

Fig. 6. Justification of using the branching *B*-factor instead of LCB*f* for polymer LCB study. MW(B) = 2 × MW(A), Branching B_n (A) = 1, and B_n (B) = 2, therefore LCB*f* (B) = LCB*f* (A). (See explanation in Text).

but number of branching, the *B*-values of the two samples are different. Therefore, sample B will have a higher coil size contraction effect than sample A. Furthermore, the rheological properties of the two samples would be very different. Sample A being a star-branched polymer, the LCB in sample A will have much less effect on polymer viscoelastic properties, as compared to the H-branched structure of the sample B. Although having the same LCB*f* value as sample A, the H-branched sample B is expected to have much longer rheological relaxation time, and higher elastic components than sample A of the star-branched type [31].

Also shown in Fig. 5, the LCB*f* values calculated from MALS and IV do not correlate well with gpcBR either. As discussed in the earlier session, LCB*f* based on R_g calculation from MALS contains both precision and accuracy problems. The precision problem was demonstrated in Section 1 and in Fig. 2, where the different formalisms and fitting orders provides inconsistency R_g values. Then there is this accuracy problem caused by the late-elution phenomenon, shown in Fig. 3. The effect of late elution situation is an overestimate of R_g in low to medium molecular weight region that can cause the determined LCB from GPC-MALS lower than it should be, as shown here in Fig. 5.

Another polymer selected for this LCB study is a set of HDPE samples with low level LCB. A commercial HDPE was transformed into this set of branched test samples of gradually increasing LCB by multi-cycle extrusion. Previous study has shown that LCB in this HDPE sample was increasingly generated with the increasing number of extrusion cycles [15]. The GPC information and calculated B_{Total} of these samples with 5 different LCB levels is shown in Table 2.

Fig. 7 demonstrates that in this HDPE series, the branching on main chain is the dominating factor that influences the gpcBR index, much more than that from the branch on branch. In this system, LCB*f* from $g_{est,gpcBR}$ increases with increasing gpcBR, because the backbone molecular weight was not significantly changed by multiple extrusion in this series of HDPE samples. Similar trend was observed on LCB*f* determined from GPC-IV, where the structure factor ε was assumed to be 1.1. Increasing number of branching also increase the frequency. However, the LCB*f* calculated from R_g from MALS cannot distinguish the LCB differences among all the samples.

3.4. Comparison of $B_{Total,\ GPC}$ and $B_{Total,\ NMR}$

In order to test the accuracy of branching number from this g_{est} concept, ^{13}C-NMR 500 MHz with cryogenic 10-mm probe was used to measure LCB. The method and calculation was explained in Rungswang's work in 2016 [21]. As shown in Fig. 8, the total branching number from both techniques are nearly the same at low LCB levels, then the deviation starts at higher level of LCB. This

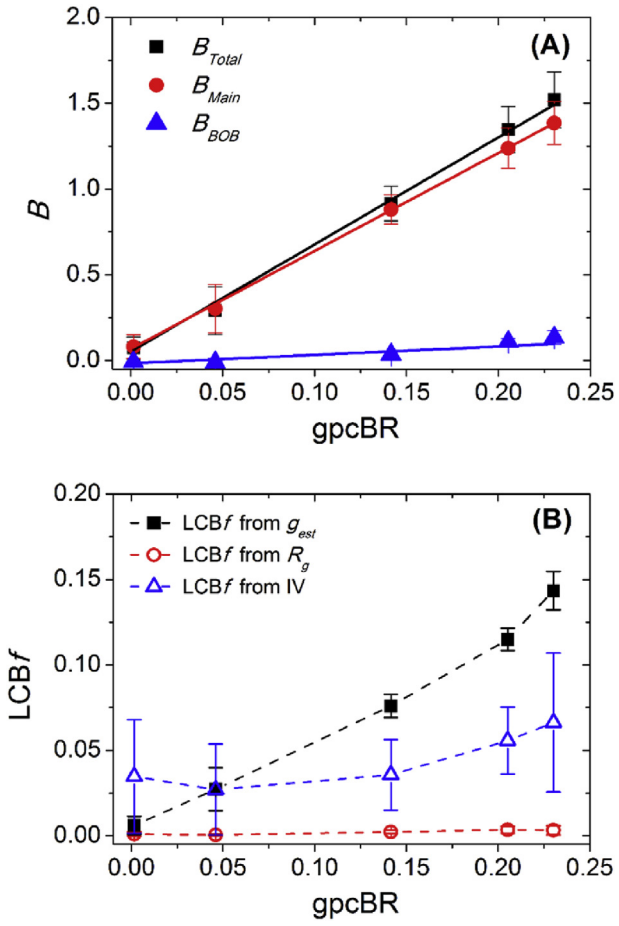

Fig. 7. (A) Branching number (*B*), **(B)** LCB*f* from three different methods and gpcBR relationship of HDPE with gradual increase of LCB by multiple extrusion.

Table 2
GPC data[a] and calculated parameters from HDPE samples.

Sample	gpcBR Eq. 6	$M_{W,CC}$ (Kg/mol)	$M_{W,ABS}$ (Kg/mol)	$g_{est,gpcBR}$ Eq. 16	B_{Total} Eq. 4	LCB*f* -$g_{est,gpcBR}$ Eq. 18	LCB*f*-R_g Eqs. (1), (4) and (5)	LCB*f*-IV Eqs. (2)–(5)
HD-1	0.00	192	166	1.00	0.07	0.01	0.0010	0.0348
HD-2	0.05	160	149	0.97	0.29	0.03	0.0005	0.0270
HD-3	0.14	165	171	0.92	0.92	0.08	0.0023	0.0358
HD-4	0.21	159	174	0.88	1.35	0.11	0.0035	0.0558
HD-5	0.23	140	157	0.87	1.52	0.14	0.0033	0.0663

[a] Data were averaged from 4 repetitions. Standard deviations are shown in Plots in Fig. 7(A) and (B).

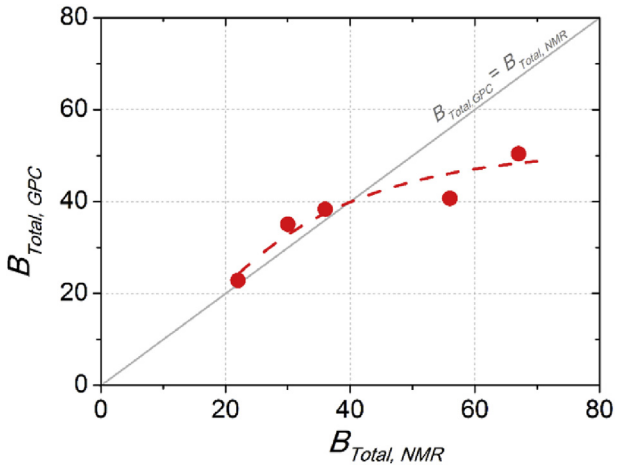

Fig. 8. Comparison of total branching number from GPC-3D with g_{est} method and from ^{13}C-NMR.

results can be discussed with the following possible contributing factors. With this GPC method, the SCB was not taken into account, leading to extra LCB level. As well as in NMR, the LCB was determined from all branches that possess higher than 6 Carbon atoms. So, the LCB number from NMR could be higher than that from GPC. At high LCB level, the additional discrepancy would result from the GPC point of view. The free volume space in polymer coil decreases with increasing LCB. The segmental excluded volume effect increases with increasing LCB. That can cause the highly branched molecules to appear larger than they would be without the excluded volume effect. The coil expansion caused by increasing excluded volume effect could cause an underestimate of the true LCB level. Another reminder needs to be noted. The ^{13}C-NMR technique for determining LCB has its limitation at detecting the very low level of LCB [17].

3.5. Relationship of B and processing properties

An example of processing property that relates to long chain branching number is die swell ratio, which can be done in a simple experiment in the laboratory scale. A sample with high LCB is expected to provide higher elasticity and presents larger die swell ratio. Fig. 9 shows that die swell ratio of LDPE increases with increasing number of LCB, which can refer to the increasing elasticity in polymer. As shown in Fig. 9, the number of branches on main chain, B_{Main}, can more strongly affect the die swell ratio value than B_{BOB}; when a slight increase in B_{Main} can make a large enhancement of die swell ratio value. This evidence supports the expected rheological behavior, where the branches on main chain are long enough and able to entangle with other molecules. They can enhance the extensional processing performance of polymers [31].

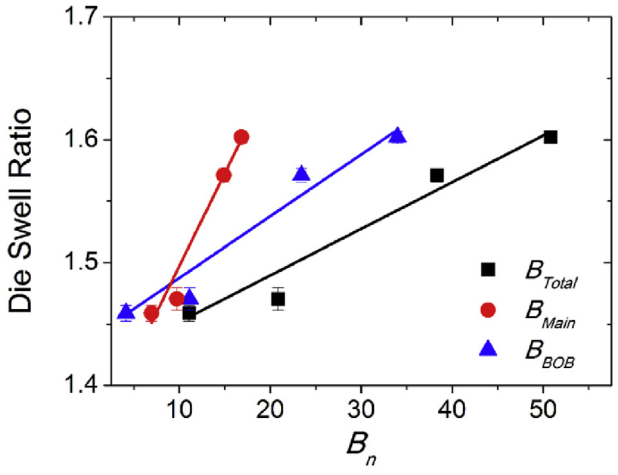

Fig. 9. Relationship of number of LCB of LDPE with die swell ratio.

4. Summary

The precision and accuracy problem of R_g determination from GPC-MALS was here demonstrated, while there was much less problem in its absolute molar mass determination. This makes it difficult to use R_g from MALS to study polymer LCB. In this report, an alternative method based on the Flory-Fox theory was developed to estimate R_g ($R_{g,est}$) by using more reliable parameters of [η] and $M_{W,ABS}$ from GPC-3D. The method was expanded to provide a more reliable branching *g*-factor, g_{est}. The method can also allow a g_{est} calculation based on the gpcBR approach. Both approaches provided comparable g_{est} results. Two sets of samples are used in this study, one is a set of highly branching LDPE, and the other one is a set of HDPE samples having low level of LCB. Branching number was determined via Zimm-Stockmayer random LCB model, and analyzed in three categories. i.e., the total number of branches (B_{Total}), number of branches on main chain (B_{Main}), and number of branches on branches (B_{BOB}). The number of LCB from GPC-3D with g_{est} approach agrees reasonably well with the LCB number from ^{13}C-NMR. All branching numbers of the LDPE samples relate nicely to the processing properties; i.e. die swell ratio. The main effect of LCB can be here identified as the following. Branches on main chain backbone provide more influence on the polymer processing properties than that of the branch-on-branch type. This is a nice confirmation to what is expected from rheological theory.

Unlike most other publications on LCB study using 3D-GPC, the emphasis of this report is focused on the branching number *B* factor rather than the branching frequency factor LCB*f*. The reason to use the *B*-factor not LCB*f* to study LCB is explained with the support of experimental data and theoretical consideration.

Acknowledgements

The authors would like to acknowledge SCG Chemicals Co., Ltd. for financial support, and thank LDPE product development team for LDPE samples and property information.

References

[1] D. Yan, W.-J. Wang, S. Zhu, Effect of long chain branching on rheological properties of metallocene polyethylene, Polymer 40 (7) (1999) 1737–1744.
[2] V.C. Barroso, J.M. Maia, Influence of long-chain branching on the rheological behavior of polyethylene in shear and extensional flow, Polym. Eng. Sci. 45 (7) (2005) 984–997.
[3] A. Honkanen, C. Bergström, E. Laiho, Influence of low density polyethylene quality on extrusion coating processability, Polym. Eng. Sci. 18 (13) (1978) 985–989.
[4] S. Kouda, Prediction of processability at extrusion coating for low density polyethylene, Polym. Eng. Sci. 48 (6) (2008) 1094–1102.
[5] P. Tackx, J.C.J.F. Tacx, Chain architecture of LDPE as a function of molar mass using size exclusion chromatography and multi-angle laser light scattering (SEC-MALLS), Polymer 39 (14) (1998) 3109–3113.
[6] C.P. Lusignan, T.H. Mourey, J.C. Wilson, R.H. Colby, Viscoelasticity of randomly branched polymers in the vulcanization class, Phys. Rev. E 60 (5) (1999) 5657–5669.
[7] S. Grcev, P. Schoenmakers, P. Iedema, Determination of molecular weight and size distribution and branching characteristics of PVAc by means of size exclusion chromatography/multi-angle laser light scattering (SEC/MALLS), Polymer 45 (1) (2004) 39–48.
[8] W.-J. Wang, S. Kharchenko, K. Migler, S. Zhu, Triple-detector GPC

characterization and processing behavior of long-chain-branched polyethylene prepared by solution polymerization with constrained geometry catalyst, Polymer 45 (19) (2004) 6495–6505.
[9] A.M. Striegel, Mid-chain grafting in PVB-graft-PVB, Polym. Int. 53 (11) (2004) 1806–1812.
[10] W. Radke, A.H.E. Müller, Synthesis and characterization of comb-shaped polymers by SEC with on-line light scattering and viscometry detection, Macromolecules 38 (9) (2005) 3949–3960.
[11] Y. Yu, P.J. DesLauriers, D.C. Rohlfing, SEC-mals method for the determination of long-chain branching and long-chain branching distribution in polyethylene, Polymer 46 (14) (2005) 5165–5182.
[12] F.J. Stadler, V. Karimkhani, Correlations between the characteristic rheological quantities and molecular structure of long-chain branched metallocene catalyzed polyethylenes, Macromolecules 44 (13) (2011) 5401–5413.
[13] S. Ahn, H. Lee, S. Lee, T. Chang, Characterization of branched polymers by comprehensive two-dimensional liquid chromatography with triple detection, Macromolecules 45 (8) (2012) 3550–3556.
[14] I. Suárez, B. Coto, Determination of long chain branching in PE samples by GPC-MALS and GPC-VIS: comparison and uncertainties, Eur. Polym. J. 49 (2) (2013) 492–498.
[15] T. Pathaweeisariyakul, K. Narkchamnan, B. Thitisak, W. Yau, Methods of long chain branching detection in PE by triple-detector gel permeation chromatography, J. Appl. Polym. Sci. 132 (28) (2015) 42222.
[16] B.H. Zimm, W.H. Stockmayer, The dimensions of chain molecules containing branches and rings, J. Chem. Phys. 17 (12) (1949) 1301–1314.
[17] A.M. Striegel, M.R. Krejsa, Complementarity of universal calibration SEC and 13C NMR in determining the branching state of polyethylene, J. Polym. Sci. Part B Polym. Phys. 38 (23) (2000) 3120–3135.
[18] P. Kratochvíl, M. Netopilík, On the contraction factors of long-chain branched macromolecules, Eur. Polym. J. 51 (2014) 177–181.
[19] F. Beer, G. Capaccio, L.J. Rose, High molecular weight tail and long-chain branching in low-density polyethylenes, J. Appl. Polym. Sci. 80 (14) (2001) 2815–2822.
[20] W.W. Yau, Examples of using 3D-GPC-TREF for polyolefin characterization, Macromol. Symp. 257 (1) (2007) 29–45.
[21] W. Rungswang, K. Narkchamnan, N. Pecharat, B. Thitisak, T. Pathaweeisariyakul, Primitive structure and its morphology for describing highly-branched structure of low-density polyethylene, Polym. Bull. (2016).
[22] S. Podzimek, Light Scattering, Size Exclusion Chromatography and Asymmetric Flow Field Flow Fractionation - Powerful Tools for the Characterization of Polymers, Proteins, and Nanoparticles, John Wiley & Sons, Inc., Hoboken, New Jersey, 2011, pp. 219–231.
[23] P.J. Flory, T.G. Fox, Treatment of intrinsic viscosities, J. Am. Chem. Soc. 73 (5) (1951) 1904–1908.
[24] O. Ptitsyn, Y.E. Eizner, Hydrodynamics of polymer solutions. 2. Hydrodynamic properties of macromolecules in active solvents soviet, Phys. Tech. Phys. 4 (9) (1960) 1020–1036.
[25] H.L. Wagner, C.A.J. Hoeve, Mark-houwink relations for linear polyethylene in 1-Chloronaphthalene and 1,2,4-Trichlorobenzene, J. Polym. Sci. Part B Polym. Phys. 11 (6) (1973) 1189–1200.
[26] S. Podzimek, Light Scattering, Size Exclusion Chromatography and Asymmetric Flow Field Flow Fractionation - Powerful Tools for the Characterization of Polymers, Proteins, and Nanoparticles, John Wiley & Sons, Inc., Hoboken, New Jersey, 2011, pp. 318–330.
[27] S. Podzimek, Light Scattering, Size Exclusion Chromatography and Asymmetric Flow Field Flow Fractionation - Powerful Tools for the Characterization of Polymers, Proteins, and Nanoparticles, John Wiley & Sons, Inc., Hoboken, New Jersey, 2011, pp. 233–234.
[28] M. Gaborieau, R.G. Gilbert, A. Gray-Weale, J.M. Hernandez, P. Castignolles, Theory of multiple-detection size-exclusion chromatography of complex branched polymers, Macromol. Theory Simul. 16 (1) (2007) 13–28.
[29] D. Konkolewicz, A.A. Gray-Weale, R.G. Gilbert, Molecular weight distributions from size separation data for hyperbranched polymers, J. Polym. Sci. Part A Polym. Chem. 45 (14) (2007) 3112–3115.
[30] F. Vilaplana, R.G. Gilbert, Characterization of branched polysaccharides using multiple-detection size separation techniques, J. Sep. Sci. 33 (22) (2010) 3537–3554.
[31] R.G. Larson, Combinatorial rheology of branched polymer melts, Macromolecules 34 (13) (2001) 4556–4571.